AADE
AMERICAN ASSOCIATION
of DRILLING ENGINEERS

Acidizing High Temperature Carbonate Reservoirs Using Methanesulfonic Acid: A Coreflood Study

Alexis Ortega and Hisham A. Nasr-El-Din, Texas A&M University; Shawn Rimassa, BASF Corporation

Abstract

Hydrochloric acid (HCl) is the most commonly used stimulation fluid for high-temperature wells drilled in carbonate reservoirs. However, the high reaction rate of HCl with carbonate rocks and high corrosion rate on well tubulars make its use in deep wells non-viable. The current study introduces the novel application of methanesulfonic acid (MSA), a strong organic acid, to increase the permeability of carbonate formations. Demonstration of the effectiveness of MSA in generating wormholes in carbonate cores will offer the petroleum industry with an alternative system to HCl for stimulating high-temperature carbonate formations.

Coreflood studies were conducted at 250°F using limestone cores and a 10 wt%-MSA aqueous solution. A constant injection rate was maintained, and the differential pressure through the core was measured until acid breakthrough. Collected samples of the effluent fluids were analyzed using inductively coupled plasma (ICP), and a computed tomography (CT) scan of each core was performed after the acid injection.

MSA was found effective in creating wormholes in limestone cores at a temperature of 250°F. At low injection rates, face dissolution and conical channels were observed in the cores. At intermediate injection rates, no face dissolution appeared and the tendency was to create a few dominant wormholes. At high injection rates, several ramified wormhole structures were found. For the conditions tested, an optimum flow rate was identified. This paper summarizes the results obtained and the recommendations for the use of MSA in carbonate acidizing applications.

Introduction

Hydrochloric acid (HCl) is generally selected for carbonate acidizing because it reacts readily with carbonate minerals producing soluble reaction products, and it is available in large quantities at a relatively low price. The main disadvantage of HCl is its high corrosivity on wellbore tubular goods, especially at temperatures above 250°F (Williams et al. 1979). Another limitation of the use of HCl is its negative environmental impact. HCl is toxic to aquatic life by lowering the pH and is not expected to biodegrade when it is released into the soil.

There are numerous problems associated with the high corrosion rate of HCl at high temperatures. First, well tubulars are often made of low-carbon steel, but in certain applications the well completion may include aluminum- or chromium-plated components (i.e., 13% chromium tubulars suitable for applications involving CO_2 rich environments) that become easily damaged upon contact with HCl solutions (Nasr-El-Din et al. 2003). In addition, HCl will dissolve any rust present in the tubulars and produce a great quantities of iron (Fe^{+3}), which will precipitate as $Fe(OH)_3$ (Crowe 1985; Taylor et al. 1999) or, if H_2S is present, as iron sulfide (Nasr-El-Din et al. 2002), potentially causing formation damage.

Various additives, such as corrosion inhibitors and inhibitor aids, are used to reduce corrosion by HCl at high temperatures. The cost of these additives, however, may result in the treatment being uneconomical (Fredd 1997). Also, the use of corrosion inhibitors in high concentrations may result in undesired wettability changes of the formation as the inhibitor may adsorb on the rock surface (Schechter 1992). These drawbacks make organic acids attractive for stimulating high-temperature wells.

Organic acids are typically used as an alternative to HCl in high-temperature formations (Chatelain et al. 1976; Van Domelen and Jennings 1995; Fredd and Fogler 1998a; Huang et al. 2000; Nasr-El-Din et al. 2001; Al-Katheeri et al. 2002; Buijse et al. 2004; Alkhaldi et al. 2009; Nasr-El-Din et al. 2013). These acids are less corrosive and spend slower in carbonate rock than HCl, thus providing deeper penetration and improved stimulation. Therefore, they are preferred when the treating temperature prevents efficient protection against corrosion and/or when the treatments are limited to low injection rates to avoid fracturing the formation. In contrast to these advantages, Chang et al. (2008) listed some limitations associated with the use of weak organic acids: they cannot be used at high acid concentration, they have a low dissociation constant, their degree of hydrogen ion generation decreases with an increase in temperature, and their cost is significantly higher than that of HCl for an equivalent mass of rock dissolved.

Some methods, including the use of sulfonic acids, have been tried in an effort to overcome the drawbacks for both mineral and conventional organic acid systems used in carbonate stimulation. Sulfonic acids, which have the formula RSO_3H, are described as a group of organic acids that contain one or more sulfonic, $–SO_3H$, groups (Tully 2000). Although the R-group may be derived from many different sources,

typical R-groups are alkane, alkene, alkyne, and arene. Sulfonic acids are such strong acids (as strong as sulfuric acid) that they dissociate completely in water (King 1991). The obtained pK_a value for MSA is -1.92 (Covington and Thompson 1974). As seen in **Table 1**, sulfonic acids are stronger than conventional organic acids but not as strong as HCl. Because of their unique chemical and physical properties, sulfonic acids have found wide application in the chemical and pharmaceutical industries, and more recently in the oilfield.

One of the first references of the potential use of alkanesulfonic acids for the treatment of oilfield wells is found in a patent filed by Tate (1982), who disclosed a method for improving the recovery of hydrocarbons in sandstone formations. More recently, Fu (2010) proposed the injection of an aqueous mixture for the treatment of sandstone formations, which consisted of a surfactant, an inorganic acid (for example HCl), and an organic acid (such as formic acid, acetic acid, citric acid, or MSA). In a similar application, Fuller (2010) presented a method for treating sandstone formations which consisted of injecting a blend of an aqueous liquid, a fluoride source, and an effective amount of an alkane sulfonic acid, preferably MSA. The stimulation of carbonate formations using alkanesulfonic acids, and in particular MSA, was first disclosed by Heidenfelder et al. (2009). In a more recent publication, Bertkau and Steidl (2012) disclosed an innovative method comprising the use of alkanesulfonic acid (MSA) microcapsules as an additive for carbonate acidizing applications. None of the previous studies found in literature included a description of the wormholing characteristics of sulfonic acids (and specifically, MSA) when they are injected through carbonate cores at high temperature conditions.

A coreflood study was conducted to determine the effectiveness of MSA in creating wormholes during the stimulation or carbonate reservoirs. MSA was found able to generate wormholes when it was injected through limestone cores at 250°F. From the study, an optimum acid injection rate was identified, and the effect of the generated dissolution patterns on acid efficiency was analyzed.

Background on Optimum Injection Rate

Wormholes are deep, highly ramified dissolution channels formed by the reaction of acid with porous carbonate rocks. The control of the formation of these channels, which are an order of magnitude larger in diameter than the naturally occurring pores, is important for the success of stimulation treatments (Hill and Schechter 2000). When evaluating the performance of a newly proposed acid system or comparing its properties to commonly used acids, the characterization of these dissolution patterns is required.

In order to understand the wormholing process, many theoretical models have been developed (Buijse and Glasbergen 2005; Daccord et al. 1989; Economides et al. 2013; Furui et al. 2012a, 2012b; Hoefner and Fogler 1988; Hung et al. 1989; Pichler et al. 1992). One of the main challenges of these models is the determination of the dissolution pattern as a function of acid injection rate. Daccord et al. (1989), for example, defined three domains of dissolution patterns as functions of flow rate:

compact (stable) dissolution at low flow rates, wormhole (unstable) domain at intermediate flow rates, and uniform dissolution (homogeneous etching) at high flow rates.

In addition to the theoretical models, numerous laboratory studies have shown a dependency of the efficiency of acidizing treatments on the generated dissolution pattern. This observation has resulted in the concept of an "optimum injection rate" (Fredd and Fogler 1998a; Hoefner and Fogler 1989; Wang et al. 1993).

The optimum flow rate is defined as the acid injection rate corresponding to the minimum volume of acid required for wormhole breakthrough. This optimum rate has been found to be determined by the dissolution pattern created by the acid reaction, and therefore is a function of rock composition, acid concentration, reaction temperature, core length, and formation permeability (Bazin 2001; Fredd and Fogler 1999; Wang et al. 1993).

Identifying the optimum injection rate for a given rock/acid system is critical for the comprehension of the wormholing mechanisms. This is a base parameter for the design (selection of acid concentration, acid volume, and injection rate) of acid treatments. Therefore, it is necessary to determine the optimum injection rate for the new stimulation fluid (MSA) in carbonate rocks.

Experimental Procedures

Laboratory coreflood experiments were conducted with Indiana limestone core samples and 10 wt% MSA. The experiments were performed at a temperature of 250°F. An overburden pressure of 1,800 psi was applied to the core cell by means of a manual hydraulic pump connected to the coreflood setup. A new core was used for each experiment.

The acid was injected into the core at a constant flow rate until breakthrough was observed. A minimum pressure of 1,100 psi was maintained in the core by a backpressure regulator downstream of the core. This pressure was required to prevent a separate CO2-rich phase from forming.

During acid injection, samples of the effluent were collected and analyzed for pH, calcium concentration, and post-treatment acid concentration. An Orion PrepHecT Ross Electrode was used to measure the pH value of the samples. The calcium concentration and final acid concentration in the core effluent samples were determined by using the inductively coupled plasma (ICP) and the Titrando 907 equipment, respectively. Finally, after the acid injection, computed tomography (CT) scans of the core samples were performed to characterize the generated wormholes.

Materials

The acid solutions were prepared using commercially available Baso® MSA (70 wt% MSA) and corrosion inhibitor BASF-JJ-103, both of which were provided by BASF. The water used throughout the experiments was deionized water with a resistivity of 18.2 MΩ•cm at room temperature.

Acid Preparation

The MSA was obtained at an initial concentration of 70 wt%. For the experimental procedure, the acid was diluted to a concentration of 10 wt% (MSA10) using deionized water. Corrosion inhibitor at a concentration of 2 vol% was added to the diluted acid solution.

Core Preparation

Core samples, from a block of Indiana limestone, were cut into cylinders of 1.5-in. diameter and 6-in. length. The samples were dried in an oven at a temperature of 250°F for 8 hours and then weighed. After this, the samples were saturated in water under vacuum conditions for 24 hours and weighed. From the difference in weight of the dry and saturated core samples, the average porosity was calculated and found to be in the range of 13.7 to 17.0%.

Before the acid injection, the core samples were placed inside the core holder, and deionized water was injected at different flow rates (5, 10, and 20 cm^3/min). The pressure drop across the cores at each flow rate was recorded, and Darcy's law was used to determine the initial (absolute) permeability of the cores. **Table 2** summarizes the properties of the cores used.

Coreflood Setup

The coreflood setup (**Fig. 2**) was used to test the performance of the new organic acid system. A pressure transducer was connected to a computer with LabView®* software installed to monitor and record the pressure drop across the core during the experiments. A Teledyne ISCO D-series D1000 precision syringe pump with a maximum allowable working pressure of 2,000 psi was used to inject the acid into the core.

To heat the core to the required test temperature, a heat jacket was placed around the core holder.The temperature was controlled by a compact bench top CSC32 series with a 4-digit display and a 0.1° resolution with an accuracy of ±0.25% full scale ±1°C. It uses a type-K thermocouple and two outputs (5 A 120 Vac SSR). Water was injected at 2 cm^3/min during the heating period.

Experimental Procedures

Seven coreflood runs were performed using 10 wt% MSA, at injection rates from 1 to 20 cm^3/min. These runs were done to test the effect of the injection rate on MSA performance, specifically, the acid volume to breakthrough, and the resulting wormhole characteristics. All the experiments were executed at a temperature of 250°F. **Table 3** presents a summary of the results obtained for each of the core samples used. During coreflood injection, the pressure drop across the core was plotted using the LabView® software. Samples of the coreflood effluent were collected and analyzed for calcium concentration, pH, and final acid concentration (acid titration).

*A registered trademark of National Instruments

The analyses performed for Core 1 (5 cm^3/min) are provided as an example of the complete coreflood procedure. **Fig. 3** shows the behavior of the pressure drop across the core during the injection of the 10 wt% MSA system at a rate of 5 cm^3/min. The differential pressure, which initially stabilized at 7.5 psi during the injection of water, started to decrease shortly after the acid injection began. This decrease in pressure indicates the reaction of the acid with the carbonate rock, and the creation of dissolution patterns (wormholes) as the acid front was moving along the core length. The differential pressure continued to decrease with time until acid breakthrough occurred.

The volume of acid to breakthrough is defined as the volume of acid needed to propagate the wormhole through the length of the core. When breakthrough was achieved, a low and constant (stable) pressure drop was recorded from the coreflood apparatus, indicating that the fluid was flowing through the created wormhole structures. For the current case, 3.27 pore volumes (PV) of acid were needed to achieve breakthrough (Fig. 3) when 10 wt% MSA was injected at 5 cm^3/min through a limestone core at 250°F.

As MSA reacted with the carbonate rock creating dissolution channels along the core, the calcium concentration in the effluent samples started to increase. **Fig. 4** shows the calcium concentration in the effluent samples, as measured by the ICP equipment, corresponding to the coreflood experiment described in Fig. 2. It shows that the total measured calcium concentration reached a maximum value of 21,595 mg/l ± 4%. This value is in agreement with the maximum theoretical value that can be calculated for a 10 wt% MSA solution (21,700 mg/l).

Fig. 5 shows the pH and final acid concentration of the coreflood effluent samples for the same experiment. The pH was around 7 at the start of the injection (water). Then it decreased with the injection of acid to a value of 1.0 (after acid breakthrough) and increased again as the injection of water restarted. As expected, an opposite trend was found for the final acid concentration on the effluent samples, which achieved a maximum value of 1.15 wt% MSA after acid breakthrough. This indicated that the acid was almost completely spent after its flow through the carbonate core.

To observe the effect of the acid on the inlet and outlet sides of the core and to identify dissolution structures created by the acid reaction with the limestone rock, photographs of the core sample were taken before and after the acid injection (**Fig. 6**). This figure shows that, for intermediate injection rates (5 cm^3/min), several pores for wormhole initiation were present, without dissolution of the inlet face of the core. Since this rate is close to the optimum, a few dominant wormholes of intermediate size were created.

A procedure similar to the one explained above for Core 1 was followed for all the other core samples used in the study (Table 2). **Fig. 7** shows the behavior of the pressure drop across the core during the injection of the 10 wt% MSA system at injection rates of 1.5, 10, and 20 cm^3/min. As described above, in each case the differential pressure decreased with time as wormholes were created until acid breakthrough was achieved.

Fig. 8 presents the ICP measured calcium concentrations in the coreflood effluent samples, collected for some of the experiments at different injection rates. As in the case of Core 1, the calcium concentration increased with the injection of acid, reaching a maximum value, then decreased when the injection fluid was switched back to water.

The calcium concentration is related to the amount of carbonate rock dissolved by acid, and this amount is greater for greater acid/rock contact times/area. Consequently, the highest peak for calcium concentration was noticed at injection rates of 1 and 20 cm^3/min (the least optimal cases, highest contact time/area), while the lowest peak was observed at injection rates of 7.5 cm^3/min (the most optimal case, lowest contact time).

Similarly, the change in pH can be compared for all the cases tested (**Fig. 9**). The decrease in pH to a minimum value indicates acid breakthrough, therefore it can be used to confirm the breakthrough determined from the analysis of the pressure drop. This minimum value of pH varied in the range of 0.97 (Core 8, 20 cm^3/min) to 1.87 (Core 32, 1 cm^3/min). The results in Fig. 9 also demonstrate the dependency of pH on injection rate. The higher the acid injection rate, the lower the time the acid has for spending upon contact with the carbonate rock, therefore resulting in lower pH of the effluent samples.

Optimum Injection Rate

The optimum injection rate is the rate at which the volume of acid required to achieve breakthrough is minimum. The volume of acid to breakthrough as a function of interstitial velocity is shown in **Fig. 10**. From this figure, as the injection rate increases, the volume of acid to breakthrough decreases and reaches a minimum at a rate between 5 and 7.5 cm^3/min (2.6 to 3.9 cm/min). At injection rates higher than the optimum, the volume of acid to achieve breakthrough increases again. However, the curve is steeper on the left side of the optimum injection rate and relatively flat for rates higher than the optimum. This fact indicates that the effect of the injection rate is more pronounced at low injection rates, corresponding to a mass-transfer-limited regime. On the other hand, a surface-reaction-limited regime is reached for high injection rates, with the pore volumes to breakthrough being affected less by changes in injection rate.

A figure similar to Fig. 10 can be constructed by plotting, as a function of interstitial velocity, the photographs of the inlet side of the core samples after acid injection (**Fig. 11**). This is done to observe the dissolution patterns obtained at each flow rate, which will govern the shape of the optimum injection rate curve. As mentioned before, the optimum injection rate is determined by the dissolution patterns created by the acid reaction.

As seen in Fig. 11, at low injection rates (1 cm^3/min), some degree of face dissolution, as well as conical wormholes, is present in the core sample making the acidizing process (wormhole penetration) significantly inefficient. As the injection rate is increased for intermediate flow rates (from 5 to 10 cm^3/min), almost no face dissolution appears on the core

sample, and the tendency is to create a few dominant wormholes.

The lowest volume of acid to breakthrough is obtained when acid is injected at 7.5 cm^3/min, and therefore, for the conditions tested, this is considered the optimum injection rate when 10 wt% MSA is injected through limestone cores at a temperature of 250°F. Finally, for high injection rates (above 10 cm^3/min), several dominant wormholes were created with increased wormhole branching as flow rate increased.

CT Scan Images

The dissolution structures that were created at the different flow rates considered in the coreflood study can be characterized by analyzing the 2D scan images of the cores treated with 10 wt% MSA. **Fig. 12** (top) presents the CT scan images for a low-injection case (Core 2, 2 cm^3/min), showing the wormholing ability of MSA at this injection rate. Dissolution of the inlet face of the core can be observed in the initial images (dark spots in the images as a result of a low CT number). A conical wormhole is also visible, which caused the core stimulation to be inefficient (sub-optimal).

Fig. 12 (bottom), on the other hand, shows the 2D scan images for a case close to the optimum rate (Core 3, 7.5 cm^3/min), on which no face dissolution of the core was observed; additionally, a single dominant wormhole was created, penetrating the total length of the core. The size of the generated wormhole decreased as the acid penetrated deeply into the core, until acid breakthrough was achieved. This dissolution pattern resulted in an efficient stimulation of the core.

Analysis of the 2D scan images provides an explanation for the difference in calcium concentration measured for both the low injection rate case and the near-optimum rate case, described in a previous section. At a low injection rate (2 cm^3/min), a large volume of MSA is consumed on the inlet flow face of the core (face dissolution). Also at this rate, the reactant penetrates into the porous matrix and enlarges flow channels. However, a significant amount of MSA is consumed on the walls of these flow channels, causing the formation of a conical-shaped dissolution channel. This conical channel requires the injection of several pore volumes of acid for the channel to break through the porous medium. The combined effect of face dissolution and conical channels results in a high degree of acid reaction with the rock, which in turn generates a high amount of calcium ions in the effluent samples.

On the other hand, at an intermediate injection rate (7.5 cm^3/min) unconsumed MSA reaches the tip of the growing flow channels. Successive consumption at the tip extends the dissolution channels and leads to the development of a dominant wormhole of reduced size. This dominant wormhole requires a minimum pore volume of acid to break through the rock matrix. For that reason, the calcium concentration of the effluent samples at this intermediate rate is lower than the corresponding concentration for the low injection rate case.

From the study of the 2D scan images it is confirmed that MSA can be used as an effective stimulation fluid at intermediate flow rates, being able to create deep, dominant

wormholes without face dissolution. The generation of a dominant wormhole provides a significant increase in permeability, as shown in **Fig. 13**, which describes the permeability enhancement obtained in carbonate cores tested with MSA at different injection rates, after acid breakthrough occurred.

During coreflood testing, the pressure drop across the rock is measured as dissolution progresses, and the average permeability of the rock is calculated using Darcy's law. It can be observed from results in Fig. 13 that the amount of acid required to increase the average permeability by a certain factor depends on the acid injection rate. For example, at a very low injection rate (i.e., 1 cm^3/min), the average permeability increases slowly with the pore volumes of acid injected. As the acid injection rate is increased, the rate of increase in average permeability increases up to a certain acid injection rate (7.5 cm^3/min). At this acid-injection rate, the optimum injection rate, permeability increment is steepest as compared with other acid-injection rates. For acid-injection rates (i.e., 20 cm^3/min) higher than the optimum acid-injection rate, the rate of permeability increment decreases with the increase in the injection rate.

Conclusions

MSA is a suitable alternative stimulation fluid for carbonate acidizing at high temperatures (250°F). A 10 wt% MSA aqueous acid solution was used to stimulate limestone cores using a coreflood setup. Based on the results obtained, the following conclusions can be drawn:

1. MSA was found to be effective in creating wormholes in limestone cores at different injection rates and at a temperature of 250°F. At low injection rates (lower than 1.5 cm3/min), face dissolution and conical channels were observed in the cores. At intermediate injection rates (5 to 10 cm3/min), almost no face dissolution appears on the core samples, and the tendency is to create a few dominant wormholes. At high injection rates (above 10 cm3/min), several dominant wormhole structures were found with increased branching for increased flow rates.
2. For the acid injection rates covered in the current study, an optimum injection rate between 5.0 and 7.5 cm3/min was determined when MSA (10 wt%) was used to stimulate limestone cores at 250°F.
3. From ICP analysis of the effluent samples, a maximum calcium ion concentration of about 22,000 mg/l was determined. This is in agreement with the maximum calcium theoretical dissolution for 10 wt% MSA.

Acknowledgments

References

1. Al-Katheeri, M.I., Nasr-El-Din, H.A., Taylor, K.C. et al. 2002. Determination and Fate of Formic Acid in High Temperature Acid Stimulation Fluids. Presented at the International Symposium and Exhibition on Formation Damage Control, held in Lafayette, Louisiana, 20-21 February 2002. SPE-73749-MS.
2. Alkhaldi, M.H., Nasr-El-Din, H.A., and Sarma, H.K. 2009. Application of Citric Acid in Acid Stimulation Treatments. Presented at the Canadian International Petroleum Conference, held in Calgary, Alberta, 16 - 18 June 2009. PETSOC-2009-015.
4. Bazin, B. 2001. From Matrix Acidizing to Acid Fracturing: A Laboratory Evaluation of Acid/Rock Interactions. SPE Production & Operations 16 (1): 22-29. SPE-66566-PA.
5. Bertkau, W. and Steidl, N. 2012. Alkanesulfonic Acid Microcapsules and Use Thereof in Deep Wells, US 2012/0222863 A1, Sep. 6, 2012. United States: BASF SE.
6. Buijse, M., Boer, P.d., Breukel, B. et al. 2004. Organic Acids in Carbonate Acidizing. SPE Production & Operations 19 (3): 128-134. SPE-82211-PA.
7. Buijse, M.A. and Glasbergen, G. 2005. A Semiempirical Model to Calculate Wormhole Growth in Carbonate Acidizing. Presented at the SPE Annual Technical Conference and Exhibition, held in Dallas, Texas, 9-12 October 2005. SPE-96892-MS.
8. Chang, F.F., Nasr-El-Din, H.A., Lindvig, T. et al. 2008. Matrix Acidizing of Carbonate Reservoirs Using Organic Acids and Mixture of Hcl and Organic Acids. Presented at the SPE Annual Technical Conference and Exhibition, held in Denver, Colorado, USA, 21-24 September 2008. SPE-116601-MS.
9. Chatelain, J.C., Silberberg, I.H., and Schechter, R.S. 1976. Thermodynamic Limitations in Organic-Acid/Carbonate Systems. Society of Petroleum Engineers Journal 16 (4): 189-195. SPE-5647-PA.
10. Covington, A. and Thompson, R. 1974. Ionization of Moderately Strong Acids in Aqueous Solution. Part Iii. Methane-, Ethane-, and Propanesulfonic Acids at 25°C. Journal of Solution Chemistry 3 (8): 603-617.
11. Crowe, C.W. 1985. Evaluation of Agents for Preventing Precipitation of Ferric Hydroxide from Spent Treating Acid. Journal of Petroleum Technology 37 (4): 691-695. 00012497.
12. Daccord, G., Touboul, E., and Lenormand, R. 1989. Carbonate Acidizing: Toward a Quantitative Model of the Wormholing Phenomenon. SPE Production Engineering 4 (1): 63-68. SPE-16887-PA.
13. Economides, M.J., Hill, A.D., Ehlig-Economides, C. et al. 2013. Carbonate Acidizing Design. In Petroleum Production Systems, Second edition, Prentice Hall. 438-467.
15. Fredd, C.N. 1997. The Influence of Transport and Reaction of Wormhole Formation in Carbonate Porous Media: A Study of Alternative Stimulation Fluids. 9825217 Ph.D., University of Michigan.
16. Fredd, C.N. and Fogler, H.S. 1998a. Alternative Stimulation Fluids and Their Impact on Carbonate Acidizing. SPE Journal 3 (1): 34-41. SPE-31074-PA.
17. Fredd, C.N. and Fogler, H.S. 1998b. Influence of Transport and Reaction on Wormhole Formation in Porous Media. American Institute of Chemical Engineers.AIChE Journal 44 (9): 1933.
18. Fredd, C.N. and Fogler, H.S. 1999. Optimum Conditions for Wormhole Formation in Carbonate Porous Media: Influence of Transport and Reaction. SPE Journal 4 (3): 196-205. SPE-56995-PA.
19. Fu, D. 2010. Self-Diverting Pre-Flush Acid for Sandstone, US 7,666,821 B2, Feb. 23, 2010. United States: Schlumberger

Technology Corporation.

20. Fuller, M.J. 2010. Method for Treating a Subterranean Formation, US 7,753,123 B2, Jul. 13, 2010. United States: Schlumberger Technology Corporation.

21. Furui, K., Burton, R.C., Burkhead, D.W. et al. 2012a. A Comprehensive Model of High-Rate Matrix-Acid Stimulation for Long Horizontal Wells in Carbonate Reservoirs: Part I--Scaling up Core-Level Acid Wormholing to Field Treatments. SPE Journal 17 (1): pp. 271-279. SPE-134265-PA.

22. Furui, K., Burton, R.C., Burkhead, D.W. et al. 2012b. A Comprehensive Model of High-Rate Matrix-Acid Stimulation for Long Horizontal Wells in Carbonate Reservoirs: Part Ii--Wellbore/Reservoir Coupled-Flow Modeling and Field Application. SPE Journal 17 (1): pp. 280-291. SPE-155497-PA.

23. Guthrie, J.P. 1978. Hydrolysis of Esters of Oxy Acids: P K a Values for Strong Acids; Brønsted Relationship for Attack of Water at Methyl; Free Energies of Hydrolysis of Esters of Oxy Acids; and a Linear Relationship between Free Energy of Hydrolysis and P K a Holding over a Range of 20 P K Units. Canadian Journal of Chemistry 56 (17): 2342-2354.

24. Heidenfelder, T., Guzmann, M., Witteler, H. et al. 2009. Methods of Increasing Permeability in Carbonatic Rock Formations with Alkanesulfonic Acids, US 7,638,469 B2, Dec. 29, 2009. United States: BASF SE.

25. Hill, A.D. and Schechter, R.S. 2000. Fundamentals of Acid Stimulation. In Reservoir Stimulation, Third edition eds. Economides, M.J. and Nolte, K.G., Wiley Chichester. 1-28.

26. Hoefner, M. and Fogler, H.S. 1988. Pore Evolution and Channel Formation During Flow and Reaction in Porous Media. AIChE Journal 34 (1): 45-54.

27. Hoefner, M.L. and Fogler, H.S. 1989. Fluid-Velocity and Reaction-Rate Effects During Carbonate Acidizing: Application of Network Model. SPE Production Engineering 4 (1): 56-62. SPE-15573-PA.

28. Huang, T., Ostensen, L., and Hill, A.D. 2000. Carbonate Matrix Acidizing with Acetic Acid. Presented at the SPE International Symposium on Formation Damage Control, held in Lafayette, Louisiana, 23-24 February 2000. SPE-58715-MS.

29. Hung, K.M., Hill, A.D., and Sepehrnoori, K. 1989. A Mechanistic Model of Wormhole Growth in Carbonate Matrix Acidizing and Acid Fracturing. Journal of Petroleum Technology 41 (1): 59-66. SPE-16886-PA.

30. King, J.F. 1991. Acidity. In The Chemistry of Sulphonic Acids, Esters, and Their Derivatives, First edition eds. Patai, S. and Rappoport, Z., The Chemistry of Functional Groups, John Wiley & Sons. 249-260.

31. Nasr-El-Din, H., Sayed, M., Aften, C. et al. 2013. A New Organic Acid to Stimulate Deep Wells in Carbonate Reservoirs. Presented at the 2013 SPE International Symposium on Oilfield Chemistry, held in The Woodlands, TX, USA, 8 - 10 April 2013. SPE-164110-MS.

32. Nasr-El-Din, H.A., Al-Humaidan, A.Y., Fadhel, B.A. et al. 2002. Investigation of Sulfide Scavengers in Well-Acidizing Fluids. SPE Production & Operations 17 (4): 229-235. SPE-80289-PA.

33. Nasr-El-Din, H.A., Driweesh, S.M., and Muntasheri, G.A. 2003. Field Application of Hcl-Formic Acid System to Acid Fracture Deep Gas Wells Completed with Super Cr-13 Tubing in Saudi Arabia. Presented at the SPE International Improved Oil Recovery Conference in Asia Pacific, held in Kuala Lumpur, Malaysia, 20-21 October 2003. SPE-84925-MS.

34. Nasr-El-Din, H.A., Lynn, J.D., and Taylor, K.C. 2001. Lab Testing and Field Application of a Large-Scale Acetic Acid-Based Treatment in a Newly Developed Carbonate Reservoir. Presented at the SPE International Symposium on Oilfield Chemistry, held in Houston, Texas, 13-16 February 2001. SPE-65036-MS.

35. Pichler, T., Frick, T.P., Economides, M.J. et al. 1992. Stochastic Modeling of Wormhole Growth in Carbonate Acidizing with Biased Randomness. Presented at the European Petroleum Conference, held in Cannes, France, 16-18 November 1992. SPE-25004-MS.

36. Schechter, R.S. 1992. Oil Well Stimulation. Prentice Hall.

37. Tate, J.F. 1982. Aqueous Acid Solution Containing an Acrylamido Alkanesulfonic Acid Polymer, 4,332,688, Jun. 1, 1982. United States: Texaco Inc.

38. Taylor, K.C., Nasr-El-Din, H.A., and Al-Alawi, M.J. 1999. Systematic Study of Iron Control Chemicals Used During Well Stimulation. SPE Journal 4 (1): 19-24. 00054602.

39. Tully, P.S. 2000. Sulfonic Acids. In Kirk-Othmer Encyclopedia of Chemical Technology, First edition, John Wiley & Sons, Inc. 1-22.

40. Van Domelen, M.S. and Jennings, J., A. R. 1995. Alternate Acid Blends for Hpht Applications. Presented at the Offshore Europe, held in Aberdeen, United Kingdom, 5-8 September 1995. SPE-30419-MS.

41. Wang, Y., Hill, A.D., and Schechter, R.S. 1993. The Optimum Injection Rate for Matrix Acidizing of Carbonate Formations. Presented at the SPE Annual Technical Conference and Exhibition, held in Houston, Texas, 3-6 October 1993. SPE-26578-MS.

42. Williams, B.B., Gidley, J.L., and Schechter, R.S. 1979. Chapter 3. Acid Types and the Chemistry of Their Reactions. In Acidizing Fundamentals, edition, SPE Monograph Series, Henry L. Doherty Memorial Fund of AIME, Society of Petroleum Engineers of AIME. 10-18.

TABLE 1—pKₐ VALUES FOR ACIDS*		
Chemical Formula	Name	pK_a
HCl	Hydrochloric acid	-7.00
H_2SO_4	Sulfuric acid	-2.80
$C_6H_5SO_3H$	Benzenesulfonic acid	-2.80
CH_3SO_3H	**Methanesulfonic acid**	**-1.92**
$CH_3CH_2SO_3H$	Ethanesulfonic acid	-1.68
H_3PO_4	Phosphoric acid	2.12
		(pK_2=7.21)
HCOOH	Formic acid	3.75
$C(OH)(CH_2CO_2H)_2CO_2H$	Citric acid	3.13 (pK_1)
HF	Hydrofluoric acid	4.00
CH_3COOH	Acetic acid	4.77

*Data from Guthrie (1978) and Fuller (2010)

TABLE 2— CORE SAMPLES PROPERTIES (MSA)					
Core No.	Rock Type	Dry Weight, g	Saturated Weight, g	Pore Volume, cm^3	Porosity, %
32	Limestone	381.76	406.36	24.60	14.16
7	Limestone	308.64	333.71	25.07	14.43
1	Limestone	361.24	390.34	29.10	16.75
3	Limestone	363.35	392.31	28.96	16.67
4	Limestone	359.74	389.32	29.58	17.02
28	Limestone	382.77	408.49	25.72	14.80
8	Limestone	325.76	349.67	23.91	13.76

TABLE 3—SUMMARY OF COREFLOOD RESULTS (MSA)				
Core No.	Permeability, md	Injection Rate, cm^3/min	Interstitial Velocity, cm/min	Pore Vol. to Breakthrough
32	172.3	1.0	0.6	9.18
7	172.1	1.5	0.9	4.56
1	120.6	5.0	2.6	3.27
3	95.7	7.5	3.9	3.00
4	83.4	10.0	5.2	4.25
28	257.4	15.0	8.9	5.44
8	220.8	20.0	12.7	6.48
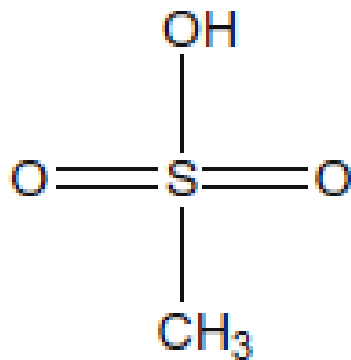
Fig. 1–Structural formula of methanesulfonic acid (MSA).
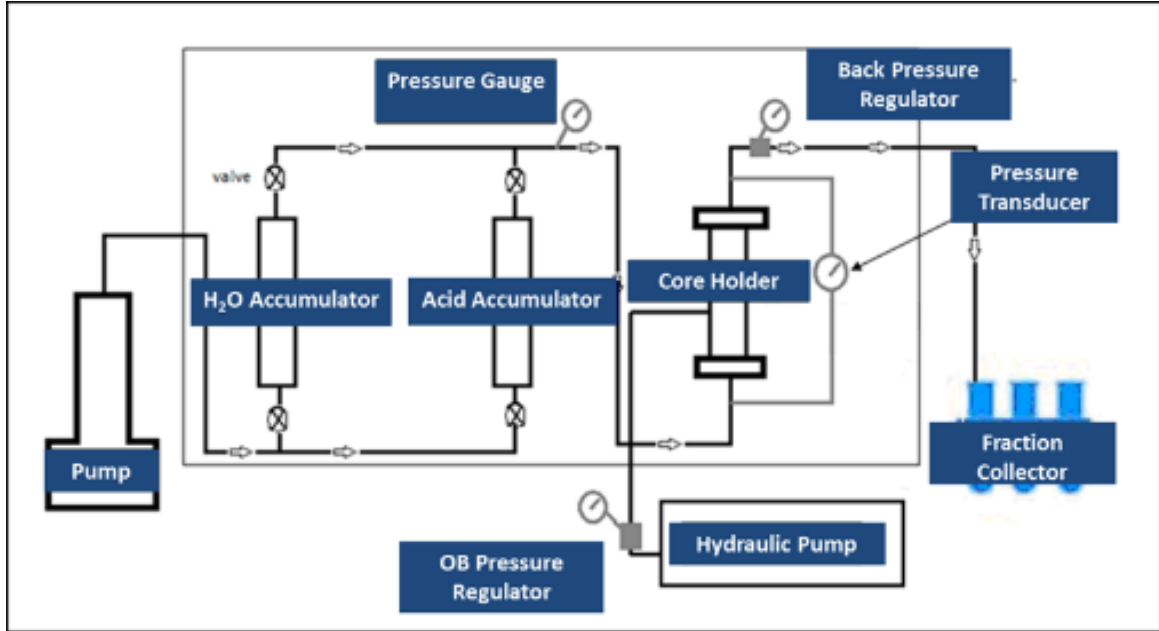
Fig. 2–Coreflood setup used to simulate matrix stimulation treatments.
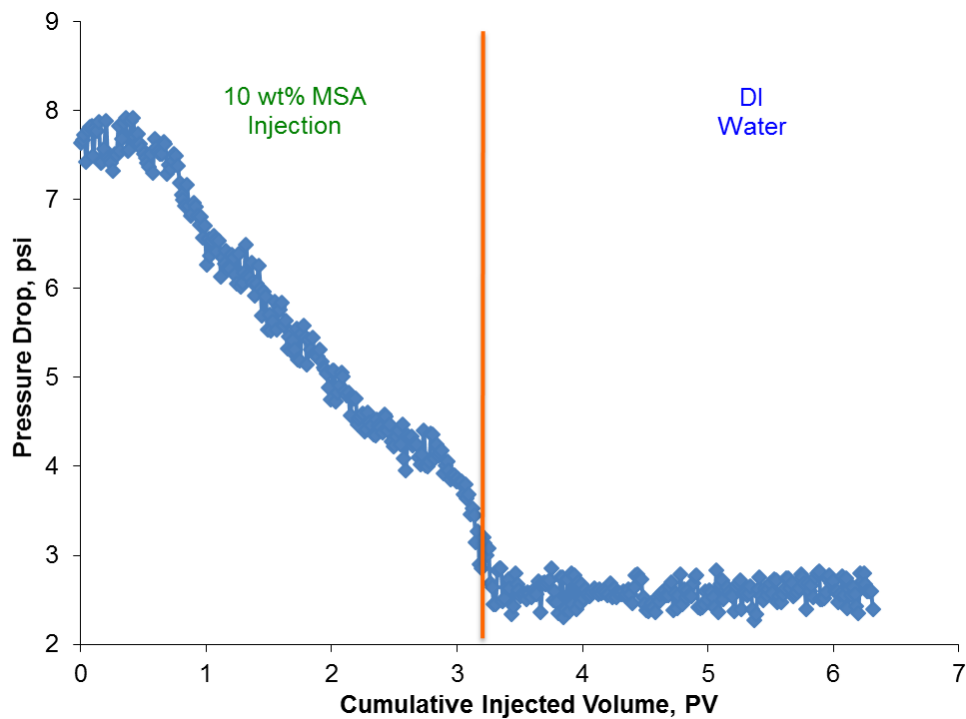
Fig. 3–Pressure drop across Core 1 during the injection of the 10 wt% MSA system at a rate of 5 cm³/min. Pressure decreased with time as wormholes were created, until acid breakthrough occurred. 3.26 PV of acid were injected.
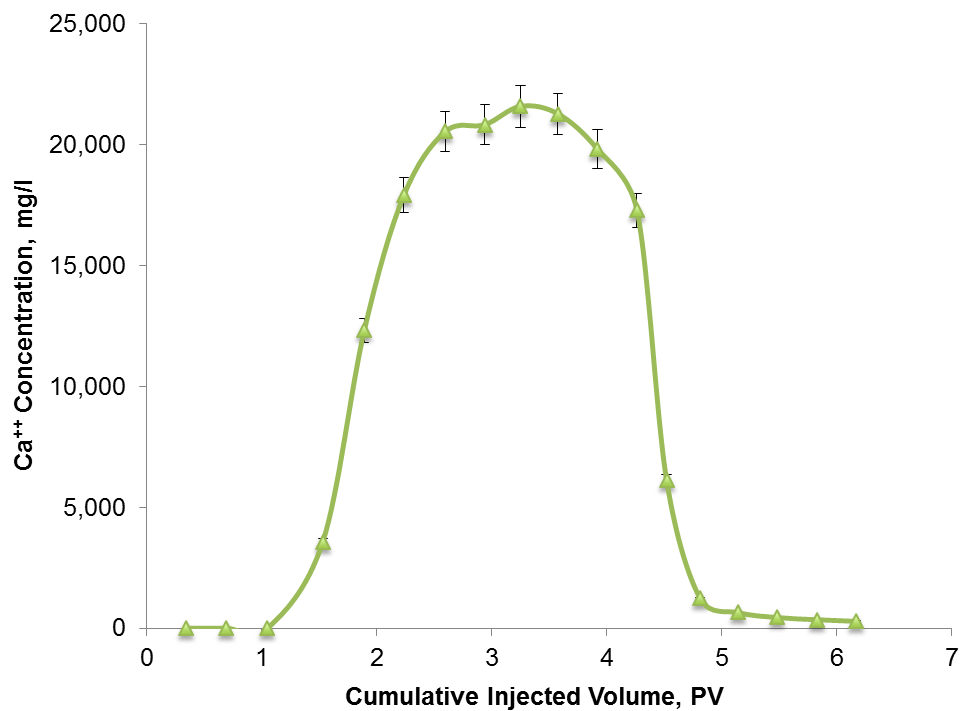
Fig. 4–Calcium concentration in the effluent samples of Core 1 from ICP equipment. A maximum value of 21,595 mg/l ± 4% was measured, which is in agreement with the theoretical value calculated for a 10 wt% MSA. Error bars represent relative standard deviation (RSD) from the measurements.
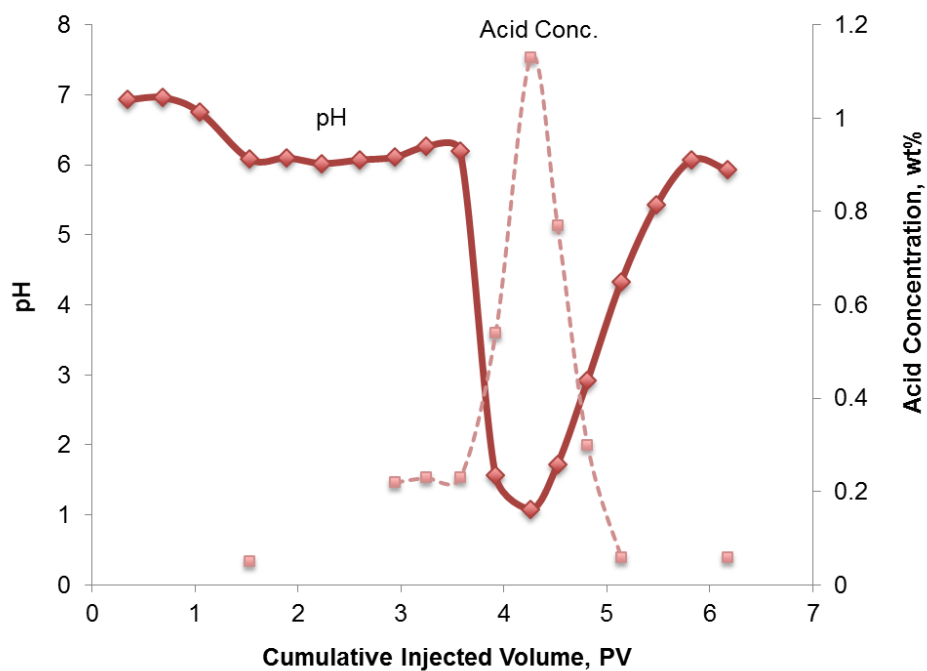
Fig. 5–pH and final acid concentration in effluent samples of Core 1. After acid breakthrough, pH reached a minimum value of 1.0, corresponding to a final acid concentration of 1.1 wt% MSA.
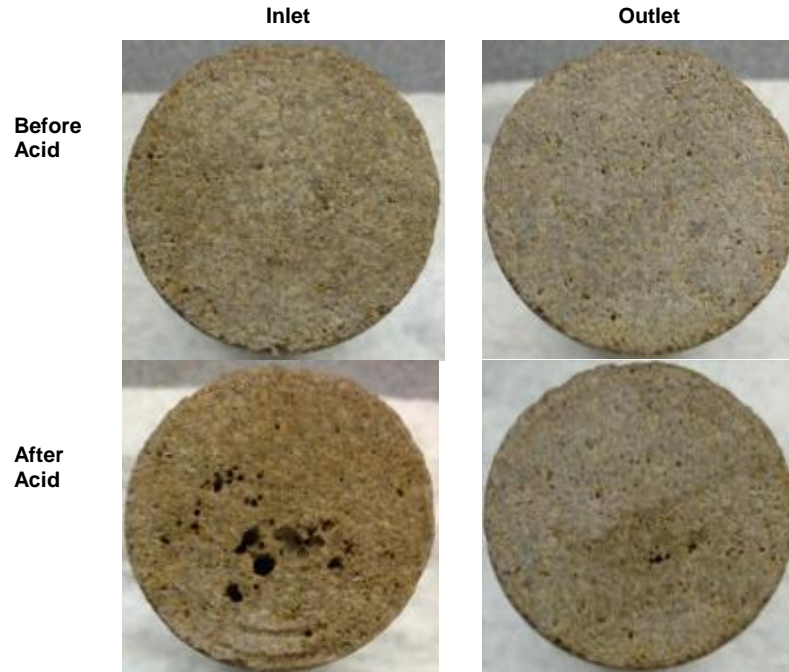
**Fig. 6–Photographs of inlet/outlet of Core 1, taken before/after acid reaction.
For intermediate injection rates (5 cm^3/min), a slight degree of face dissolution
was present with a few dominant wormholes of intermediate size.**
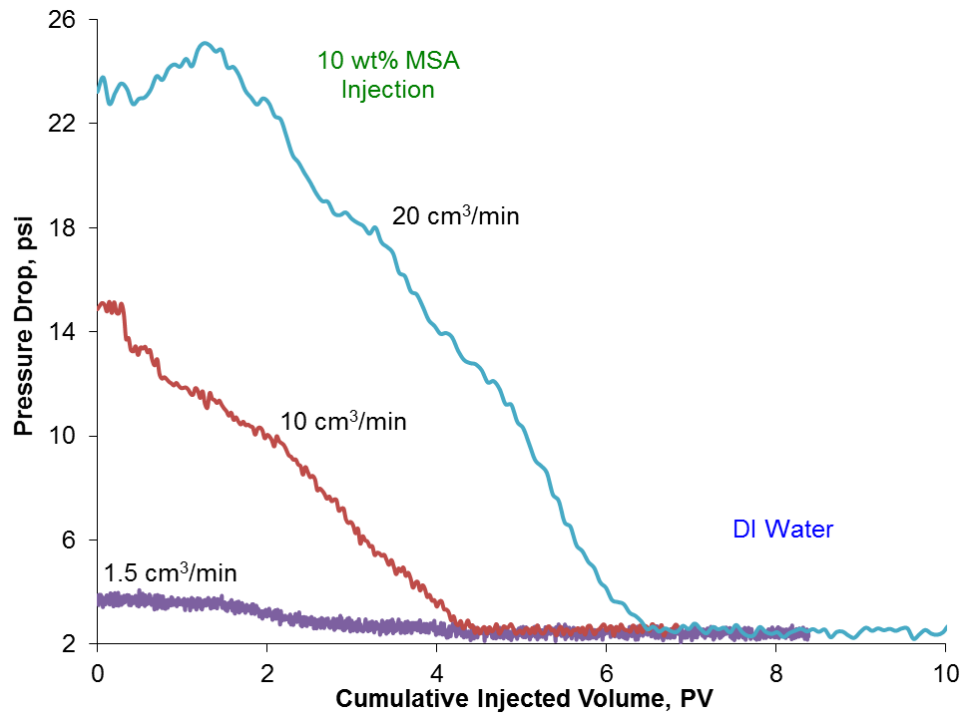
**Fig. 7–Pressure drop across different core samples during the injection of the 10 wt% MSA system at
injection rates of 1.5, 10, and 20 cm^3/min. In all cases, pressure decreased with time as wormholes were
created, until acid breakthrough was achieved.**
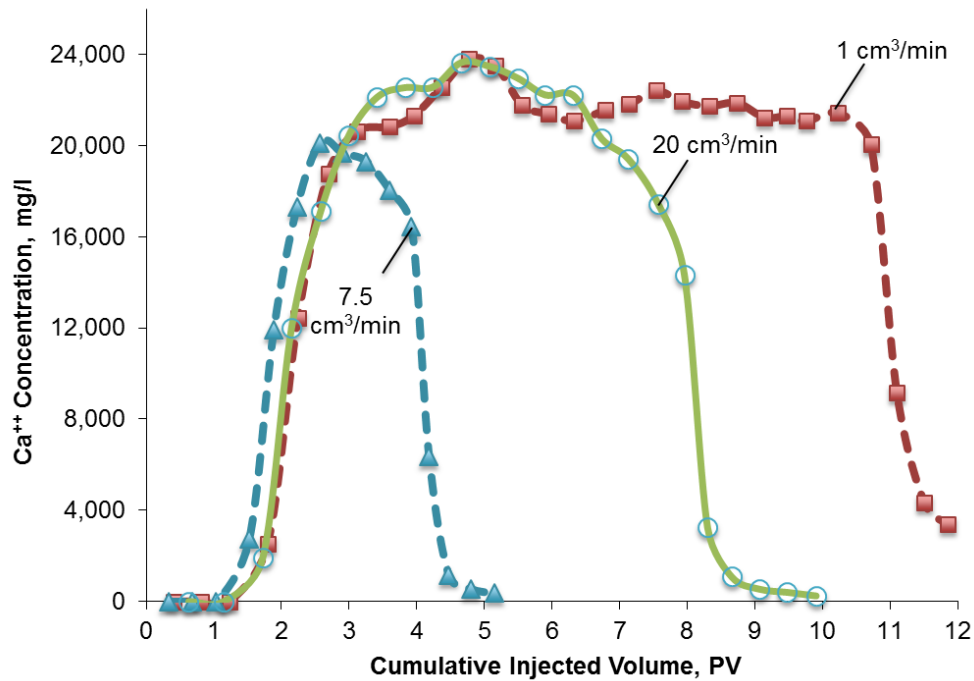
Fig. 8–Calcium concentration in the coreflood effluent samples, collected for the various experiments with MSA at different injection rates (± 4%, relative standard deviation). Highest peak for calcium concentration was found for the highest contact time cases. The lowest peak was observed for the lowest contact time cases (intermediate rates), which are closest to the optimum injection rate.
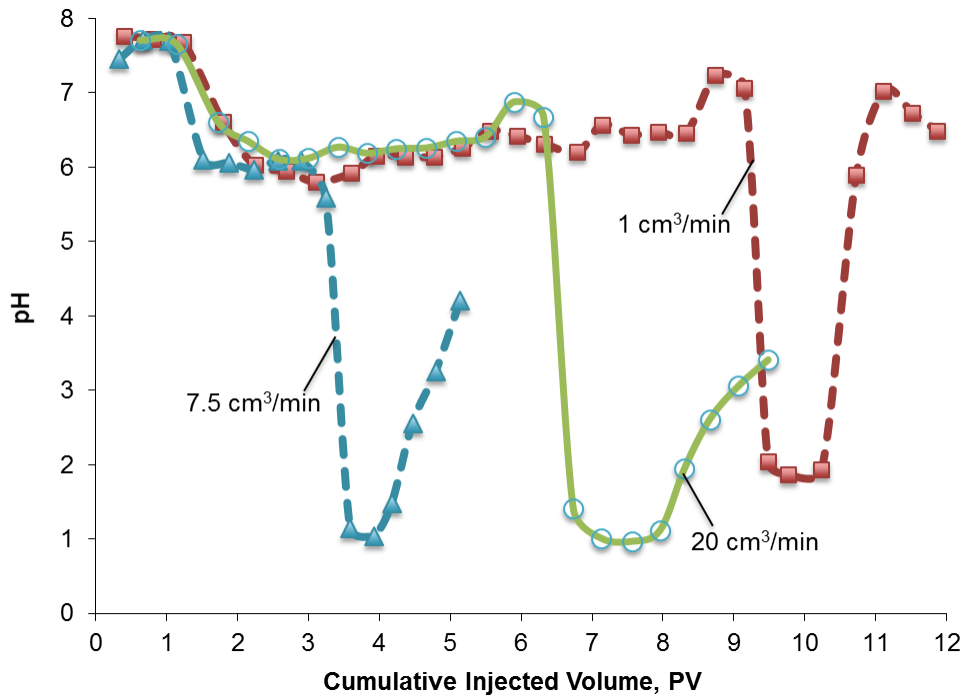

Fig. 9–pH of the coreflood effluent samples, collected for the various experiments with MSA at different injection rates. Acid breakthrough is indicated by the decrease in the pH measurement. pH measurement increases again after water injection is restarted.
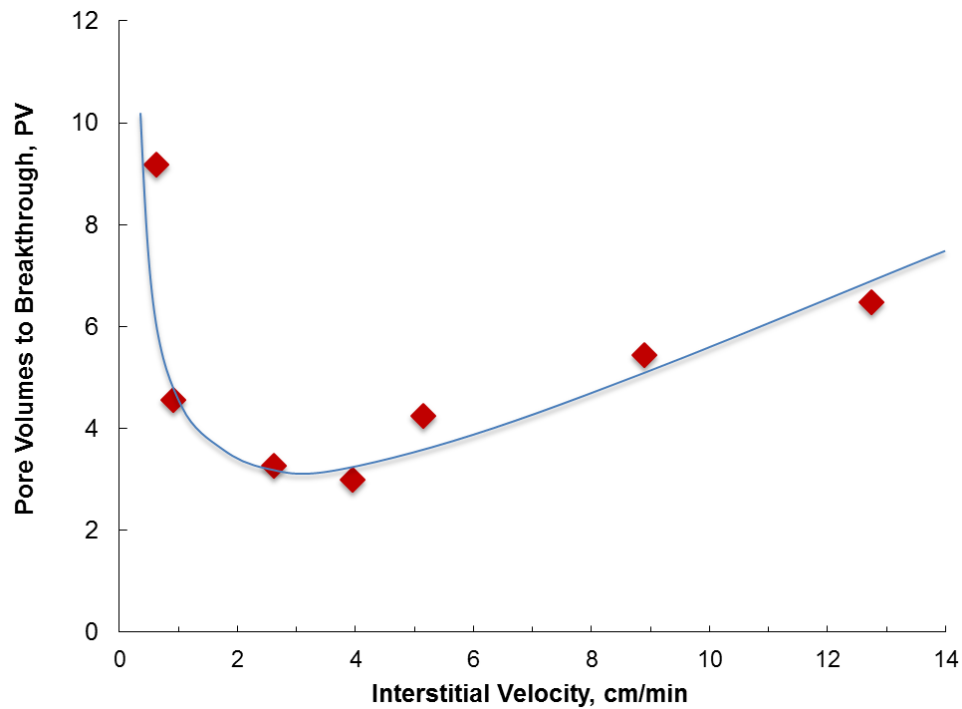
Fig. 10–Optimum injection rate curve for the reaction of MSA with limestone at 250°F. As the injection rate increased, the volume of acid to breakthrough decreased and reached a minimum at a rate between 5 and 7.5 cm³/min (2.6 to 3.9 cm/min). At injection rates higher than the optimum, the volume of acid to breakthrough increased.
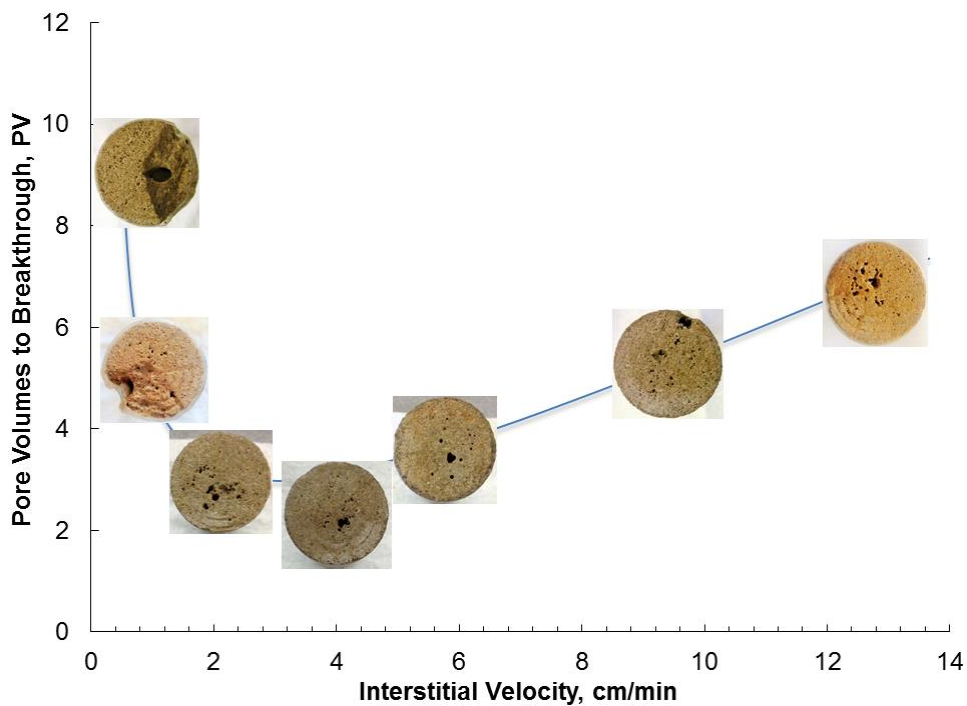

Fig. 11–Dissolution patterns after injection of 10 wt% MSA were identified from photographs of inlet side of core samples. At low injection rates, face dissolution and conical wormholes are observed. Almost no face dissolution occurs at intermediate flow rates, and single dominant wormholes are created. At high injection rates, several dominant wormholes are created with increasing branching as flow rate is increased.

CT Scan Core 2 - low-injection rate case (2 cm³/min)

CT Scan Core 3 - intermediate-injection rate case (7.5 cm³/min)
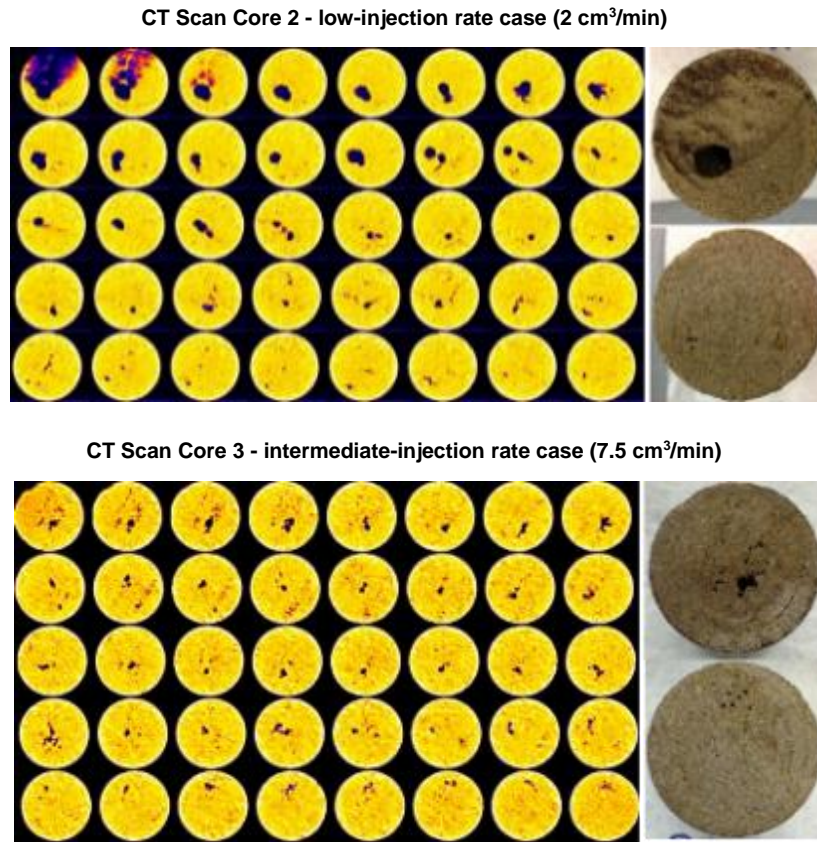
Fig. 12–Low injection (top) leads to face dissolution and conical wormholes. Dominant wormholes are a characteristic of the intermediate rate case (bottom).
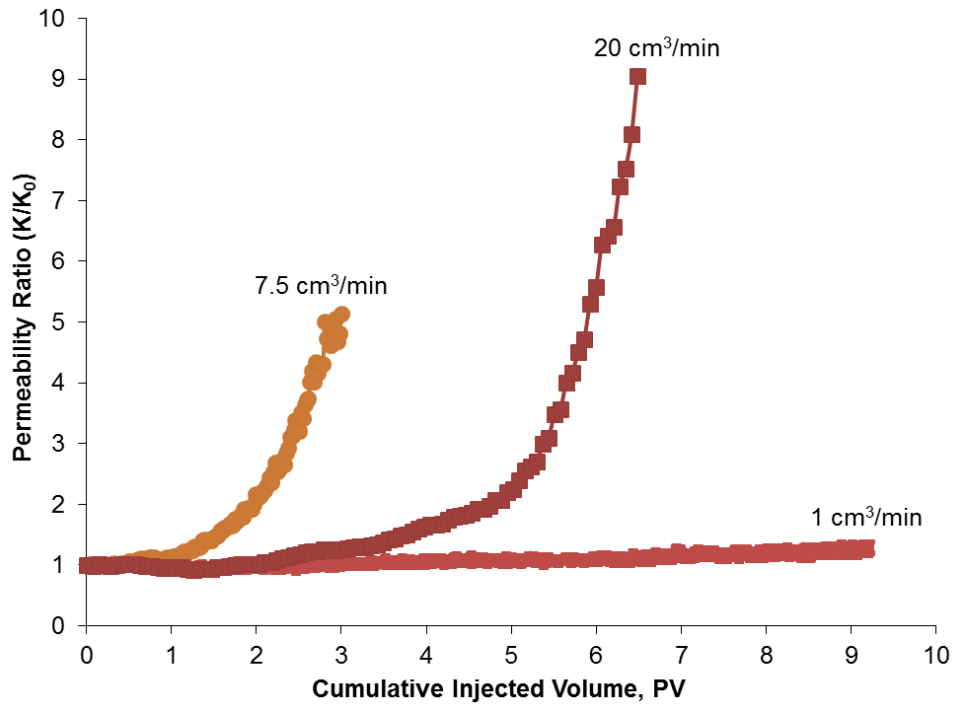
Fig. 13–Permeability enhancement by injection of 10 wt% MSA in carbonate cores. Figure shows the dependency of acid-injection rate on the amount of acid required to increase the average rock permeability by a certain factor.